Simulated Docking of Zanamivir with the 2009 Pandemic Strain Influenza A/H1N1 Neuraminidase Active Site

Jack K. Horner

Abstract

Influenza neuraminidases are glycoproteins that facilitate the transmission of the influenza virus from cell to cell. Zanamivir is a widely used neuraminidase inhibitor. Here I provide a computational docking analysis of zanamivir with the active site of the neuraminidase of the 2009 Influenza A/H1N1 strain. The computed inhibitor/receptor binding energy suggests that zanamivir would be only marginally effective against that strain.

Keywords: Influenza, H1N1, neuraminidase, zanamivir

1.0 Introduction

Influenza neuraminidases are glycoproteins that facilitate the transmission of the influenza virus from cell to cell. Zanamivir (5-(acetylamino)-2,6-anhydro-3,4,5-trideoxy-4-[(diaminomethylidene)amino]-D-glycero-D-galacto-non-2-enonic acid (4S,5R,6R)-5-acetamido-4-(diaminomethylideneamino)-6-[(1R,2R)-1,2,3-trihydroxypropyl]-5,6-dihydro-4H-pyran-2-carboxylic acid; [10]) is a widely used influenza therapeutic.

In the World Health Organization serotype-based influenza taxonomy, influenza type A has nine neuraminidase-related sero-subtypes, and these subtypes correspond at least roughly to differences in the active-site structures of the flu neuraminidases. The subtypes fall into two groups ([3]): group-1 contains the subtypes N1, N4, N5 and N8; group-2 contains the subtypes N2, N3, N6, N7 and N9. Zanamivir was designed to target the group-2 neuraminidases.

The available crystal structures of the group-1 N1, N4 and N8 neuraminidases ([1]) reveal that the active sites of these enzymes have a very different three-dimensional structure from that of group-2 enzymes. The differences lie in a loop of amino acids known as the "150-loop", which in the group-1 neuraminidases has a conformation that opens a cavity not present in the group-2 neuraminidases. The 150-loop contains an amino acid designated Asp 151; the side chain of this amino acid has a carboxylic acid that, in group-1 enzymes, points away from the active site as a

result of the 'open' conformation of the 150-loop. The side chain of another active-site amino acid, Glu 119, also has a different conformation in group-1 enzymes compared with the group-2 neuraminidases (8]).

The Asp 151 and Glu 119 amino-acid side chains form critical interactions with neuraminidase inhibitors. For neuraminidase subtypes with the “open conformation” 150-loop, the side chains of these amino acids might not have the precise alignment required to bind inhibitors tightly ([8]). The active site of the 1918 H1N1 strain has the 150-loop configuration.

The difference in the active-site conformations of the two groups of neuraminidases may also be caused by differences in amino acids that lie outside the active site. This means that an enzyme inhibitor for one target will not necessarily have the same activity against another with the same active-site amino acids and the same overall three-dimensional structure.

Crystallized Influenza A/California/04/2009(H1N1)) neuraminidase is an atypical group 1 NA with some group 2-like features in its active site (lack of a 150-cavity) ([4]).

2.0 Method

The general objective of this study is straightforward: to computationally assess the binding energy of the active site of crystallized A/California/04/2009(H1N1)) neuraminidase with zanamivir. Unless otherwise noted, all processing described in this section was performed on a Dell Inspiron 545 with an Intel Core2 Quad CPU Q8200 (clocked @ 2.33 GHz) and 8.00 GB RAM, running under the *Windows Vista Home Premium (SP2)* operating environment.

Protein Data Bank (PDB) 3TI3 ([6]) is a structural description of most of the crystallized neuraminidase of Influenza A/H1N1 3TI3 consists of two identical chains, designated Chain A and Chain B.

3TI3was downloaded from PDB on 22 February 2011. A PDB description of zanamivir was extracted from PDB 3B7E ([10]) using *AutoDock Tools* v 4.2 (ADT, [9]). ADT was then used to perform the docking of zanamivir to the receptor. More specifically, in ADT, approximately following the rubric documented in [12]

-- Chain B, and the water in Chain A, of 3TI3 were deleted

-- Chain A's active-site was extracted. (3TI3 identifies the active site of Chain A as 15 amides: ARG118, GLU119, ASP151, ARG152, ARG156, TRP178, ARG224, GLU227, SER246, GLU276, GLU277, ARG292, ASN294, ARG371, and TYR406.)

-- the hydrogens, charges, and torsions in the ligand and active site were adjusted using the ADT-recommended defaults

and finally, the ligand, assumed to be flexible wherever that assumption is physically possible, was auto-docked to the active site, assumed to be rigid, using the Lamarckian genetic algorithm implemented in ADT. The best-fit (lowest-energy) configuration from the analysis was saved, and the distances between the receptor and ligand in 3TI3, and those computed here, were compared.

The ADT parameters for the docking are shown in Figure 1. Most values are, or are a consequence of, ADT defaults.

```
autodock_parameter_version 4.2       # used by autodock to validate parameter set
outlev 1                             # diagnostic output level
intelec                              # calculate internal electrostatics
seed pid time                        # seeds for random generator
ligand_types C HD OA N               # atoms types in ligand
fld 3TI3_active.maps.fld             # grid_data_file
map 3TI3_active.C.map                # atom-specific affinity map
map 3TI3_active.HD.map               # atom-specific affinity map
map 3TI3_active.OA.map               # atom-specific affinity map
map 3TI3_active.N.map                # atom-specific affinity map
elecmap 3TI3_active.e.map            # electrostatics map
desolvmap 3TI3_active.d.map          # desolvation map
move zanamivir.pdbqt                 # small molecule
about -29.5772 12.7517 -20.6465      # small molecule center
tran0 random                         # initial coordinates/A or random
axisangle0 random                    # initial orientation
dihe0 random                         # initial dihedrals (relative) or random
tstep 2.0                            # translation step/A
qstep 50.0                           # quaternion step/deg
dstep 50.0                           # torsion step/deg
torsdof 9                            # torsional degrees of freedom
rmstol 2.0                           # cluster_tolerance/A
extnrg 1000.0                        # external grid energy
e0max 0.0 10000                      # max initial energy; max number of retries
ga_pop_size 150                      # number of individuals in population
ga_num_evals 2500000                 # maximum number of energy evaluations
ga_num_generations 27000             # maximum number of generations
ga_elitism 1                         # number of top individuals to survive to next
generation
```

```
ga_mutation_rate 0.02                # rate of gene mutation
ga_crossover_rate 0.8                # rate of crossover
ga_window_size 10                    #
ga_cauchy_alpha 0.0                  # Alpha parameter of Cauchy distribution
ga_cauchy_beta 1.0                   # Beta parameter Cauchy distribution
set_ga                               # set the above parameters for GA or LGA
sw_max_its 300                       # iterations of Solis & Wets local search
sw_max_succ 4                        # consecutive successes before changing rho
sw_max_fail 4                        # consecutive failures before changing rho
sw_rho 1.0                           # size of local search space to sample
sw_lb_rho 0.01                       # lower bound on rho
ls_search_freq 0.06                  # probability of performing local search on
individual
set_psw1                             # set the above pseudo-Solis & Wets parameters
unbound_model bound                  # state of unbound ligand
ga_run 10                            # do this many hybrid GA-LS runs
analysis                             # perform a ranked cluster analysis
```

Figure 1. ADT parameters for the docking in this study

3.0 Results

The interactive problem setup, which assumes familiarity with the general neuraminidase "landscape", took about 20 minutes in ADT; the docking proper, about 28 minutes on the platform described in Section 2.0 The platform's performance monitor suggested that the calculation was more or less uniformly distributed across the four processors at ~25% of peak per processor (with occasional bursts to 40% of peak), and required a constant 2.9 GB of memory.

Figure 2 shows the best-fit zanamivir/receptor energy and position summary produced by ADT under the setup shown in Figure 1. The estimated free energy of binding under these conditions is ~ -8.7 kcal/mol; the estimated inhibition constant, ~408 nanoMolar at 298 K.

```
MODEL        1
USER    Run = 1
USER    Cluster Rank = 1
USER    Number of conformations in this cluster = 10
USER
USER    RMSD from reference structure       = 56.144 A
USER
USER    Estimated Free Energy of Binding    =   -8.72 kcal/mol  [=(1)+(2)+(3)-(4)]
USER    Estimated Inhibition Constant, Ki   =  408.13 nM (nanomolar)  [Temperature =
298.15 K]
USER
USER    (1) Final Intermolecular Energy     =  -11.40 kcal/mol
USER        vdW + Hbond + desolv Energy     =   -8.30 kcal/mol
USER        Electrostatic Energy            =   -3.10 kcal/mol
USER    (2) Final Total Internal Energy     =   -2.75 kcal/mol
USER    (3) Torsional Free Energy           =   +2.68 kcal/mol
USER    (4) Unbound System's Energy  [=(2)] =   -2.75 kcal/mol
USER
USER
USER
USER    DPF = 3TI3_zanamivir.dpf
USER    NEWDPF move    zanamivir.pdbqt
```

```
USER    NEWDPF about   -29.577200 12.751700 -20.646500
USER    NEWDPF tran0   29.961176 14.781299 -20.419074
USER    NEWDPF axisangle0     -0.004045 -0.391949 0.919978 3.081993
USER    NEWDPF quaternion0    -0.000109 -0.010540 0.024740 0.999638
USER    NEWDPF dihe0   4.89 175.54 139.90 180.00 67.18 1.07 -179.74 0.58 -36.96
USER
USER                                x       y       z    vdW   Elec        q     RMS
ATOM      1  C2  ZMR A1001      29.610  13.398 -22.778 -0.14 +0.09    +0.144 56.144
ATOM      2  C3  ZMR A1001      30.901  13.720 -22.564 -0.34 +0.01    +0.045 56.144
ATOM      3  C4  ZMR A1001      31.277  14.664 -21.442 -0.27 -0.00    +0.150 56.144
ATOM      4  C5  ZMR A1001      30.226  14.586 -20.317 -0.17 +0.04    +0.143 56.144
ATOM      5  C6  ZMR A1001      28.817  14.747 -20.891 -0.14 +0.08    +0.185 56.144
ATOM      6  O6  ZMR A1001      28.541  13.810 -21.924 -0.14 -0.22    -0.335 56.144
ATOM      7  NE  ZMR A1001      32.576  14.369 -20.810 -0.22 +0.04    -0.217 56.144
ATOM      8  HE  ZMR A1001      32.843  13.389 -20.711 -0.26 -0.16    +0.178 56.144
ATOM      9  CZ  ZMR A1001      33.401  15.265 -20.371 +0.01 +0.06    +0.665 56.144
ATOM     10  NH1 ZMR A1001      33.240  16.579 -20.493 -0.24 +0.05    -0.235 56.144
ATOM     11  NH2 ZMR A1001      34.493  14.843 -19.724 -0.31 -0.14    -0.235 56.144
ATOM     12 2HH1 ZMR A1001      32.407  16.900 -20.987 +0.08 -0.07    +0.174 56.144
ATOM     13 1HH1 ZMR A1001      33.890  17.285 -20.148 -0.38 -0.08    +0.174 56.144
ATOM     14 2HH2 ZMR A1001      34.617  13.835 -19.630 -0.39 +0.16    +0.174 56.144
ATOM     15 1HH2 ZMR A1001      35.144  15.549 -19.378 -0.44 +0.11    +0.174 56.144
ATOM     16  N5  ZMR A1001      30.437  15.627 -19.309 -0.02 -0.20    -0.352 56.144
ATOM     17  H5  ZMR A1001      30.130  16.576 -19.525 +0.10 +0.07    +0.163 56.144
ATOM     18  C10 ZMR A1001      31.013  15.406 -18.112 -0.24 +0.22    +0.214 56.144
ATOM     19  C11 ZMR A1001      31.268  16.657 -17.329 -0.34 +0.13    +0.117 56.144
ATOM     20  O10 ZMR A1001      31.344  14.278 -17.729 -0.74 -0.41    -0.274 56.144
ATOM     21  C1  ZMR A1001      29.129  12.658 -23.951 -0.19 +0.35    +0.233 56.144
ATOM     22  O1A ZMR A1001      30.010  12.129 -24.683 -1.05 -1.46    -0.642 56.144
ATOM     23  O1B ZMR A1001      27.908  12.571 -24.177 -1.03 -1.48    -0.642 56.144
ATOM     24  C7  ZMR A1001      27.690  14.594 -19.863 -0.09 +0.13    +0.180 56.144
ATOM     25  C8  ZMR A1001      26.561  15.617 -20.084 -0.25 +0.09    +0.173 56.144
ATOM     26  O8  ZMR A1001      25.343  14.887 -20.303 -0.20 -0.19    -0.391 56.144
ATOM     27  H8  ZMR A1001      24.662  15.515 -20.514 -0.40 -0.11    +0.210 56.144
ATOM     28  C9  ZMR A1001      26.902  16.556 -21.266 -0.21 +0.02    +0.198 56.144
ATOM     29  O9  ZMR A1001      25.780  16.637 -22.140 -0.01 -0.06    -0.398 56.144
ATOM     30  H9  ZMR A1001      25.104  16.044 -21.835 -0.35 -0.03    +0.209 56.144
ATOM     31  O7  ZMR A1001      27.148  13.287 -19.968 +0.01 -0.32    -0.390 56.144
ATOM     32  H7  ZMR A1001      27.094  13.052 -20.887 +0.08 +0.19    +0.210 56.144
TER
ENDMDL
```

Figure 2. ADT's zanamivir energy and position predictions.

Figure 3 is a rendering of the active-site/inhibitor configuration computed in this study.

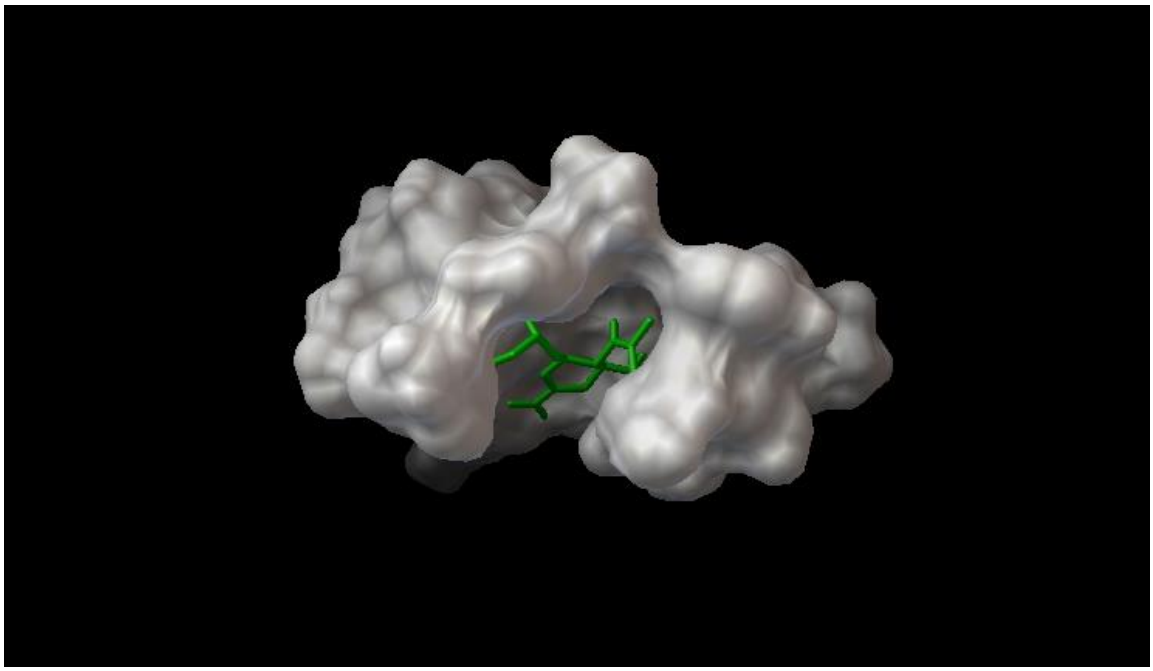

Figure 3. Rendering of zanamivir computationally docked with the active site of PDB 3TI3. The molecular surface of the receptor is shown in white; the inhibitor, in stick form in green. Only the interior, inhibitor-containing region of the molecular surface of the active site can be compared to *in situ* data: the surface distal to the interior is a computational artifact, generated by the assumption that active site is detached from the rest of the receptor.

The distances between ligand and receptor atoms in 3TI3, and the corresponding distances in the present computation were within 10% of each other.

4.0 Discussion

The method described in Section 2.0 and the results of Section 3.0 motivate several observations:

1. The inhibition constant computed in this study (~408 nanoMolar at ~298 K) is comparable inhibition constant of neuraminidase inhibitors that are not clinically effective ([10], [11], [13], [14], [15]) against several H1N1 genotypes. This suggests that zanamivir would be only marginally effective against Influenza A/California/04/2009(H1N1)). It would, however, be more effective than oseltamivir (Tamiflu®) against that strain.

2. The docking study reported here assumes that the receptor is rigid. This assumption is appropriate for the binding energy computation for PDB 3TI3 per se. However, the calculation does not reflect what receptor "flexing" could contribute to the interaction of the ligand with native unliganded receptor.

3. The analysis described in Sections 2.0 and 3.0 assumes receptor is in a crystallized form. *In situ*, at physiologically normal temperatures (~310 K), the receptor is not in crystallized form. The ligand/receptor conformation *in situ*, therefore, may not be identical to their conformation in the crystallized form.

4. Minimum-energy search algorithms other than the Lamarckian genetic algorithm used in this work could be applied to this docking problem. Future work will use Monte Carlo/simulated annealing algorithms.

5. A variety of torsion and charge models could be applied to this problem, and future work will do so.

6. 3TI3 has two chains, each with its own active site. The work described in this paper was performed on Chain A only. Chain B appears to have an active site highly similar to the Chain A active site. Future work will assess the ligand/receptor binding energies of Chains B.

5.0 Acknowledgements

This work benefited from discussions with Tony Pawlicki. For any problems that remain, I am solely responsible.

6.0 References.

[1] Russell RJ et al. The structure of H5N1 avian neuraminidase suggests new opportunities for drug design. *Nature* 443 (6 September 2006), 45-49.

[2] Johnson NP and Mueller J. Updating the accounts: global mortality of the 1918-1920 "Spanish " influenza pandemic. *Bulletin of the History of Medicine* 76 (2002), 105-115.

[3] World Health Organization. A revision of the system of nomenclature for influenza viruses: a WHO memorandum. *Bulletin of the World Health Organization* 58 (1980), 585-591.

[4] Vavricka CF, Li Q, Wu Y, Qi J, Wang M, Liu Y, Gao F, Liu J, Feng E, He J, Wang J, Liu H, Jiang H, and Gao GF. Structural and functional analysis of laninamivir and its octanoate prodrug reveals group specific mechanisms for Influenza NA inhibition. *PLoS Pathogens* 7 (October 2011): e1002249. doi:10.1371/journal.ppat.1002249.

[5] Butler D. Avian flu special: The flu pandemic: were we ready? *Nature* 435 (26 May 2005), 400-402. doi: 10.1038/435400a.

[6] PDB ID = 10.2210/pdb3ti3/pdb. See also [4].

[7] US Centers for Disease Control. *Summary: Interim Recommendations for the Use of Influenza Antiviral Medications in the Setting of Oseltamivir Resistance among Circulating Influenza A (H1N1) Viruses, 2008-09 Influenza Season.* 19 December 2008. URL http://www.cdc.gov/flu/professionals/antivirals/summary.htm.

[8] Luo M. Structural biology: antiviral drugs fit for a purpose. *Nature* 443 (7 September 2006), 37-38. doi:10.1038/443037a, published online 6 September 2006.

[9] Morris GM, Goodsell DS, Huey R, Lindstrom W, Hart WE, Kurowski S, Halliday S, Belew R, and Olson AJ. *AutoDock* v4.2. http://autodock.scripps.edu/. 2010.

[10] PDB ID = 10.2210/pdb3b7e/pdb. Xu X, Zhu X, Dwek RA, Stevens J, Wilson IA. Structural characterization of the 1918 influenza virus H1N1 neuraminidase. *Journal of Virology* 82 (2008), 10493-10501.

[11] Govorkova EA et al. Comparison of efficacies of RWJ-270201, oseltamivir, and zanamivir against H5N1, H9N2, and other avian influenza viruses. *Antimicrobial Agents and Chemotherapy* 45 (2001), 2723-2732.

[12] Huey R and Morris GM. *Using AutoDock 4 with AutoDock Tools: A Tutorial*. 8 January 2008. http://autodock.scripps.edu/.

[13] Cheng Y and Prusoff WH. Relationship between the inhibition constant (K_i) and the concentration of inhibitor which causes 50 per cent inhibition (I_{50}) of an enzymatic reaction. *Biochemical Pharmacology* 22 (December 1973), 3099–3108. doi:10.1016/0006-2952(73)90196-2.

[14] Horner JK. Simulated docking of oseltamivir with the 1918 pandemic strain Influenza A/H1N1 zanamivir-conformed neuraminidase active site. *Proceedings of the 2011 International Conference on Genetic and Evolutionary Methods*. CSREA Press. 2011. pp. 130-135.

[15] Horner JK. Simulated docking of zanamivir with the 1918 pandemic strain Influenza A/H1N1 neuraminidase active site. *Proceedings of the 2011 International Conference on Genetic and Evolutionary Methods.* CSREA Press. pp. 136-142.